A paired marine-fluvial modern pollen dataset from the Bohai Sea and its inflowing rivers, China

Jie Li[1], Shixiong Yang[1], Siyuan Ye[1], Xiangjun Meng[1], Xiaohui Chen[1], Xi Mei[1], Maosheng Gao[1], Qian Hao[2], Xiaoyong Cao[3], Bin Chen[1], Sangheon Yi[4], and Guangming Zhao[1]

[1]*Qingdao Institute of Marine Geology, China Geological Survey, Qingdao 266237, China*
[2]*Institute of Surface-Earth System Science, School of Earth System Science, Tianjin University, Tianjin 300072, China*
[3]*Group of Alpine Paleoecology and Human Adaptation (ALPHA), State Key Laboratory of Tibetan Plateau Earth System, Environment and Resources (TPESER), Institute of Tibetan Plateau Research, Chinese Academy of Sciences, Beijing 100101, China*
[4]*Korea Institute of Geoscience and Mineral Resources, Daejeon 305-350, Republic of Korea*
Correspondence: Shixiong Yang (ysx_666@163.com) and Guangming Zhao (guangming_210@163.com)

Abstract: Modern marine pollen records can be interpreted reliably only when the main source-to-sink processes between terrestrial vegetation, rivers, and marine depocentres are documented by comparable modern data. Here, we present and quality-assess a paired marine-fluvial pollen dataset for the Bohai Sea, China, consisting of 430 marine surface-sediment samples and 104 fluvial surface-sediment samples from 16 major inflowing rivers. The dataset includes sample coordinates, water depth for marine stations, river and regional identifiers, pollen and spore counts and percentages, pollen concentrations, and grain-size parameters. In total, 104 pollen and spore morphotypes were identified. Marine assemblages are dominated by arboreal pollen, especially *Pinus* (mean 59 %), whereas nearshore and river-influenced settings contain higher proportions of herbaceous taxa, particularly Chenopodiaceae/Amaranthaceae-type (mean 14 %), *Artemisia*, and Poaceae. Redundancy analysis after variance-inflation-factor screening indicates that water depth is the strongest retained predictor of marine pollen composition ($\lambda1/\lambda2 = 0.303$), followed by geographic position and sediment texture. In river samples, geographic position, water discharge, and pollen concentration together explain 20.53 % of the compositional variance. Along the 0-35 m depth interval, arboreal pollen and *Pinus* percentages increase with water depth, whereas herbaceous percentages decrease, providing an internally consistent modern analogue for distinguishing nearshore fluvial influence from more distal marine influence, where buoyant saccate pollen is enriched by a combination of atmospheric transport and hydrodynamic sorting. The dataset is intended primarily as a reusable calibration and quality-assessment resource for palaeoenvironmental studies in the Bohai-Yellow Sea region. The archived data are available at the National Tibetan Plateau Data Center (TPDC; Li and Yang, 2026; https://doi.org/10.11888/Paleoenv.tpdc.303516).

1 Introduction

Marginal seas at the land-ocean interface are important archives for Earth system research because their sediments integrate continental vegetation signals, fluvial sediment delivery, coastal hydrodynamics, surface and deeper oceanic currents, and sea-level change (Sun et al., 2001; Chen et al., 2003; Wang et al., 2014). The Bohai Sea, a shallow and semi-enclosed epicontinental sea on the East Asian continental margin, is a particularly suitable setting for developing a modern pollen source-to-sink dataset. It receives sediment from several river systems, including the Yellow River (Huanghe),

Liaohe River, Haihe River, and Luanhe River, and its surrounding catchments span a wide range of vegetation and land-use types across northern China (Qin et al., 1990; Liu et al., 2007; Wang et al., 2011; Yang et al., 2019a).

Pollen and spores preserved in marine sediments are widely used to reconstruct past terrestrial vegetation and climate, but marine pollen spectra do not represent source vegetation directly. Before burial, pollen grains are affected by differential production, atmospheric and fluvial dispersal, hydrodynamic sorting, sediment focusing, oxidation, and taxon-specific preservation (Müller, 1959; Havinga, 1984; Heusser, 1988; Brush et al., 1994; Chmura et al., 1999). These processes may amplify some taxa, such as bisaccate *Pinus*, and underrepresent others, especially taxa with lower production or more restricted dispersal pathways.

A robust interpretation of fossil pollen from marginal seas therefore requires modern calibration data that document both the receiving basin and the terrestrial or fluvial pathways by which pollen reaches it. Such datasets allow users to separate ecological information from transport and depositional biases, to define modern analogues, and to evaluate the uncertainty attached to pollen-based environmental inference (Prentice, 1980, 1985; Overpeck et al., 1985; Davis et al., 2013). Large regional pollen databases have advanced quantitative palaeoecology, and marine surface-sediment pollen (Yang et al., 2016a, 2016b, 2016c, 2019a, 2021) and alluvial pollen around the Bohai Sea (Yang et al., 2019b) have been documented separately. However, paired modern datasets that combine marine surface sediments with the inflowing rivers of the same basin within a single harmonized framework remain uncommon (Chmura and Liu, 1990; Luo et al., 2014; Yang et al., 2016a, 2019a, 2021).

Previous palynological studies of Bohai Sea surface sediments have shown that pollen distributions are structured by riverine input, basin circulation, sediment texture, and water depth, and that *Pinus* and herbaceous taxa often show opposite nearshore-offshore patterns (Wang, 1993; Yang et al., 2016a, 2016b, 2016c, 2019a, 2021). However, most earlier work focused on marine sediments alone. The pollen composition of the inflowing river systems, which constitutes a first-order control on the pollen delivered to the sea, has not been documented in a harmonized dataset with the marine samples. This gap limits the ability of users to assess fluvial filtering, aeolian input, and the degree to which river assemblages are transformed before final deposition in the marine basin.

Here we present an integrated modern pollen dataset that combines 430 marine surface-sediment samples from the Bohai Sea with 104 fluvial surface-sediment samples from 16 rivers that discharge into the basin. All samples were processed using comparable palynological and grain-size procedures, and the resulting records were harmonized taxonomically to facilitate reuse. The paired design is the principal added value of the dataset: it provides a modern reference from terrestrial and fluvial source areas to marine depositional sinks, rather than treating the marine signal in isolation.

The objectives of this data description article are to (1) document the sampling design, analytical procedures, variables, and metadata of the paired marine-fluvial dataset; (2) describe the main spatial patterns of pollen and spore assemblages in a way that helps future users evaluate data quality and representativeness; (3) quantify the dominant environmental gradients associated with pollen composition using exploratory ordination; and (4) provide usage guidance, uncertainty information, and limitations for palaeoenvironmental applications in the Bohai-Yellow Sea region.

2 Study region

The Bohai Sea (37-41° N, 117.5-122° E) is a shallow, semi-enclosed continental shelf sea in northern China. It is bounded by the Liaodong Peninsula to the east, the Shandong Peninsula to the

south, and the North China Plain to the west. The sea covers approximately 7.7 × 10^4 km^2 and has a mean water depth of about 18 m, with the greatest depths occurring in the northern Bohai Strait (Qin et al., 1990; IOCAS, 1985). It is commonly subdivided into Liaodong Bay, Bohai Bay, Laizhou Bay, the Central Basin, and the Bohai Strait, which connects the Bohai Sea with the Yellow Sea (Fig. 1).

The regional climate is controlled by the warm-temperate East Asian monsoon system. Summers are warm and humid under southeasterly monsoon winds, whereas winters are cold and dry under the influence of the Siberian-Mongolian high-pressure system. Mean annual temperature is approximately 12.6 °C, and mean annual precipitation generally ranges from 500 to 900 mm, with more than 70 % of annual rainfall occurring during the summer monsoon season (June-August) (Zhang et al., 1991; Wang, 2013). This strong seasonality affects both terrestrial pollen production and the timing of fluvial sediment and pollen delivery to the sea.

The surrounding vegetation belongs mainly to the warm-temperate deciduous broadleaved forest biome, although natural vegetation has been extensively modified by long-term agriculture and urban development. Remnant natural and semi-natural vegetation includes *Pinus tabuliformis*, *Quercus acutissima*, *Quercus variabilis*, *Betula*ceae, Ulmaceae, shrub-grassland communities dominated by *Artemisia*, Chenopodiaceae/Amaranthaceae-type, Poaceae, and Asteraceae, and halophytic coastal communities on saline-alkaline plains (Wang, 1993; Meng and Wang, 1987; Zhang, 2007). The Yellow River catchment alone integrates pollen from temperate steppe, temperate deciduous forest, and warm-temperate deciduous forest zones (Ren and Beug, 2002; Li et al., 2020).

The Bohai Sea receives terrigenous sediment from several major rivers, including the Yellow River, Liaohe River, Haihe River, Luanhe River, and numerous smaller coastal rivers (Table 1). The Yellow River is the dominant sediment supplier and has historically contributed most of the suspended sediment entering the basin (Milliman and Meade, 1983; Wang et al., 2007, 2011; Milliman and Farnsworth, 2011). Because sediment and pollen are transported together during fluvial discharge and redistributed by marine circulation, river-borne pollen is expected to be especially important in nearshore and deltaic settings.

Marine circulation is driven by the Yellow Sea Warm Current intrusion through the Bohai Strait, wind-driven coastal currents, tidal forcing, and density gradients related to freshwater discharge (Guan, 1994; Fang et al., 1999). Fine-grained muds accumulate preferentially in the Central Basin, where low-energy bottom conditions favour deposition of suspended sediment, whereas coarser deposits occur near river mouths and in tidally energetic channels (Liu et al., 2009; Youn and Kim, 2011). This bathymetric and textural gradient provides a natural framework for assessing how pollen assemblages change from river-influenced shallow sites to more distal marine depocentres.

Together, the shallow basin geometry, strong monsoonal seasonality, heterogeneous catchment vegetation, large fluvial sediment supply, and complex circulation make the Bohai Sea a useful modern laboratory for documenting pollen production, transport, deposition, and preservation across the land-sea continuum.

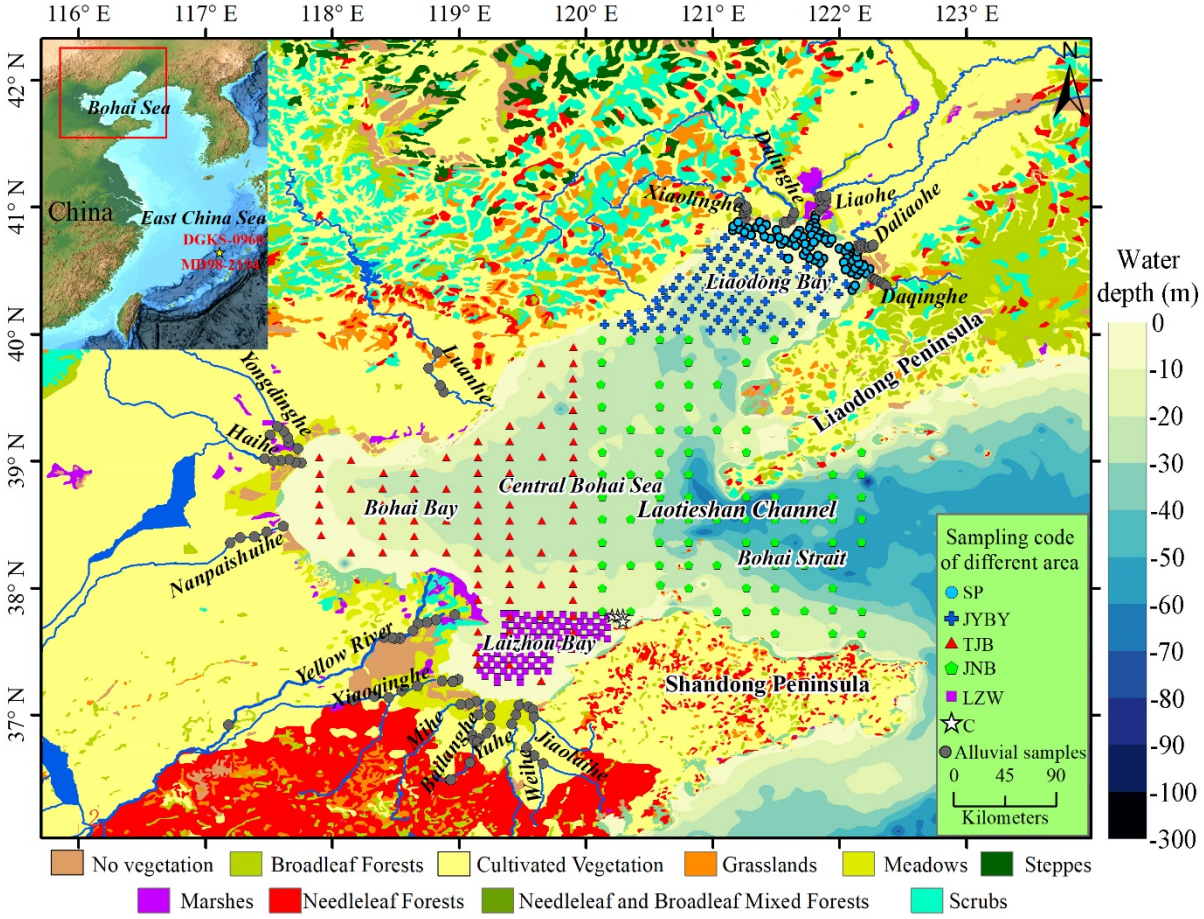

Figure 1. Sampling locations in the Bohai Sea and 16 inflowing rivers, as well as the positions of cores DGKS-9602 and MD98-2194 (Zheng et al., 2011, 2013). The vegetation background was adapted from Zhang (2007). Abbreviations for the marine sampling sites merely represent regional sampling codes, whereas symbols of different colors denote the respective areas.

Table 1. Hydrological characteristics of the main rivers discharging into the Bohai Sea. Values summarize the sources listed in the table; reporting periods differ among rivers and should be considered when comparing water discharge and sediment load.

River name	Length (km)	Area (km^2)	Water discharge (10^8 m^3 a^{-1})	Sediment load (10^4 t a^{-1})	Period	Reference
Liaohe	1396	13.65×10^4	29.35	417	1987–2010	Ministry of Water Resources of China, 2011
Dalinghe	397	23549	19.63	2740	1956-2000	Chen et al., 1998
Xiaolinghe	397.4	23549	4.03	364	/	Chen et al., 1998
Daliaohe	768.4	25360	42.21	899	1954-1979	Wang and He, 1993
Daqinghe	100.7	1482	2.82	18.49	1959-2000	Yang, 2003
Luanhe	877	4.49×10^4	46.51	1739	1950–1984	Chen et al., 1998
Haihe	1036	21.1×10^4	8.2	7.38	1990-2010	Ministry of Water Resources of China, 2011
Yongdingxinhe	61.9	8.3×10^4	0.939	17.4	/	Zhu, 2007
Nanpaishuihe	99.4	13730	4	10	/	Editorial Committee of Encyclopedia of Rivers and Lakes in China, 2014

Yellow River	5465	75.2 ×10^4	313.3	77800	1952–2010	Ministry of Water Resources of China, 2011
Weihe	242	6367	14.46	92.44	/	Chen et al., 1998
Mihe	206	3847	4.3	84.09	/	Chen et al., 1998
Xiaoqinghe	233	10498	8.78	36.9	/	Chen et al., 1998
Jiaolaihe	109	3793.5	2.33	8.7	/	Chen et al., 1998
Bailanghe	120	1237	1.22	1.16	/	Editorial Committee of Encyclopedia of Rivers and Lakes in China, 2014
Yuhe	75	301	0.05	0.82	/	Editorial Committee of Encyclopedia of Rivers and Lakes in China, 2014

3 Materials and methods

3.1 Sample collection

Surface sediments were collected from the Bohai Sea and its major inflowing rivers during field campaigns between 2010 and 2012 to establish a spatially representative modern pollen dataset (Fig. 1). The term modern is used here to denote surface sediments that integrate recent depositional conditions; users should note that the upper centimetre of marine sediment may integrate multiple years to decades depending on local sedimentation, mixing, and bioturbation rates.

The study area encompasses diverse sedimentary environments, necessitating the use of different sampling methods according to sediment type and locality. In the coastal shallow water area (water depth <5 m), surface sediments were obtained using either a boat-deployed grab sampler or a manually operated steel scoop. The grab sampler was required to retrieve no less than 1 kg (wet weight) of effective sediment, from which the upper 0–10 cm layer was carefully scraped from the central portion for subsequent laboratory analyses. In the deeper offshore areas (water depth >5 m), a box corer from research vessels was deployed to collect sediments with a depth of to 50 cm. The uppermost 10 cm mixed layer of each core was subsampled as the surface sediment fraction and stored in sample bags for further analysis. Along the inflowing rivers of the Bohai Sea, floodplain alluvium was collected as 5-cm-thick surface sediment samples using a pre-cleaned stainless steel scoop, with a sampling interval of 3–5 km. Where conditions permitted, surface sediments at a depth of 0–5 cm were additionally collected for palynological analysis.

A total of 430 marine surface sediment samples were collected. Sampling stations were more densely distributed in river-influenced areas, particularly across the Yellow River subaqueous delta and the estuarine transition zones of Bohai Bay and Laizhou Bay (Yang et al., 2016a, 2016b, 2016c). Fluvial surface-sediment samples (n = 104) were collected from 16 rivers entering the Bohai Sea: the Yellow River, Liaohe, Haihe, Luanhe, Daliaohe, Dalinghe, Xiaolinghe, Daqinghe, Yongdingxinhe, Nanpaishuihe, Xiaoqinghe, Mihe, Bailanghe, Yuhe, Weihe, and Jiaolaihe rivers. Samples were taken from lower reaches and estuarine zones, with each sample containing 100-150 g of wet sediment (Yang et al., 2019b). Floodplain and point-bar facies were targeted to capture integrated river-transported pollen, while avoiding obvious anthropogenic contamination where possible. All sampling locations were recorded using a differential GPS.

In addition, as a vast modern sink for fluvial sediments, multiple rivers, notably the Yellow River and the Luanhe River, transport enormous quantities of sediment into the Bohai Sea annually, which predominantly governs the sedimentary framework of the Bohai Bay. As a result, the surface sediments in this region are largely products of these riverine sediments that have been transported, sorted, and redeposited by marine hydrodynamic processes. Besides, small-scale tidal deposits are distributed in

the eastern Bohai Sea. The sediments of the Liaodong Shoal and Bozhong Shoal are mainly derived from the allochthonous accumulation of materials eroded by tidal currents from the Laotieshan Channel in the Bohai Strait, and represent reworked products of Late Pleistocene older strata (Liu et al., 1998).

3.2 Pollen and grain-size analysis

Prior to analysis, each sample was homogenised by thorough mixing, and representative aliquots were then withdrawn for pollen and grain-size measurements, so that both measurements derive from the same material. Pollen analysis followed standard laboratory procedures (Berglund and Ralska-Jasiewiczowa, 1986; Moore et al., 1991). For each sample, 10-20 g of dry sediment was treated sequentially with 10% HCl to remove carbonates, 40% HF to dissolve silicates, and 10 % KOH in a heated water bath to remove humic material. Samples were rinsed and centrifuged between steps. Pollen and spores were concentrated by heavy-liquid flotation using Zinc bromide ($ZnBr_2$) at a density of approximately 2.0 g mL^{-1} (Nakagawa et al., 1998). One tablet of exotic *Lycopodium* spores (27 637±563 spores per tablet) was added before chemical treatment to calculate pollen concentration (grains g^{-1} dry sediment) (Stockmarr, 1971). Pollen was identified and counted using a Nikon Eclipse Ni transmitted-light microscope at 400× magnification, with difficult grains checked at 600× or 1000× under oil immersion. Pollen residues were mounted in glycerine jelly, a mobile medium that allows the grains to be rotated and observed from different angles, which is particularly important for the identification of bisaccate grains. The target count was at least 200 terrestrial pollen-spore grains per sample; samples that did not reach this target are retained in the dataset and should be treated as low-count samples during quantitative reuse. In pollen-spore-rich samples, counts were extended beyond this minimum threshold to improve the statistical robustness of percentage estimates for less abundant taxa and to minimize the uncertainty in concentration values derived from the added *Lycopodium* marker spores. Taxonomic identifications were made using the reference collection at the Qingdao Institute of Marine Geology and published pollen atlases (Wang et al., 1995; IBSCIBAS, 1985; Tang et al., 2020). Pollen percentages were calculated from the terrestrial pollen sum, whereas fern spore percentages were calculated from the total palynomorph sum. The morphotype Chenopodiaceae/Amaranthaceae-type is retained in the manuscript to match the archived count table and common Quaternary palynological usage.

Grain-size distributions were measured by laser diffraction using a Malvern Mastersizer 2000 with a Hydro 2000G dispersion unit. Prior to measurement, samples were treated with 10% H_2O_2 to remove organic matter and 10% HCl to remove carbonates, dispersed with sodium hexametaphosphate ((NaPO3)6), and ultrasonicated. Sediments were grouped into clay (<4 μm), silt (4-63 μm), and sand (>63 μm) fractions following Wentworth (1922). Mean grain size (Mz), sorting, skewness, and kurtosis were calculated using the logarithmic method of moments implemented in GRADISTAT (Blott and Pye, 2001).

3.3 Numerical analysis

Exploratory statistical analyses were conducted in R (version 4.2.3; R Core Team, 2023), primarily with the vegan package (version 2.6-4; Oksanen et al., 2019). The purpose of these analyses was to evaluate internal pollen-environment consistency and to identify the main gradients represented in the dataset; the analyses are not intended as a formal transfer function for reconstructing past water depth or sea level.

Pollen counts were converted to relative abundances before ordination. Relative abundance data were Hellinger-transformed to reduce the influence of dominant taxa and to make the data suitable for

linear ordination (Legendre and Gallagher, 2001). Detrended correspondence analysis (DCA; Hill and Gauch, 1980) was first used to evaluate gradient lengths. The first DCA axis was 0.98 standard deviation (SD) units for the riverine dataset and 1.25 SD units for the marine dataset, both below the 3-4 SD threshold generally used to justify linear response models (ter Braak and Prentice, 1988; ter Braak and Verdonschot, 1995). Redundancy analysis (RDA) was therefore used for both datasets.

Separate RDAs were performed for riverine and marine samples. For the riverine subset, the response matrix contained 21 pollen taxa with mean relative abundance greater than 0.2 %, and predictors included latitude, longitude, pollen concentration, watershed area, mean annual water discharge, and mean annual sediment load. For the marine subset, the response matrix contained 15 pollen taxa with mean relative abundance greater than 1 %, and predictors included latitude, longitude, water depth, sand, silt, clay, mean grain size (Mz), and pollen concentration.

Environmental predictors were screened using forward selection and variance inflation factors (VIFs) to reduce multicollinearity (Blanchet et al., 2008). Variables with VIF > 10 were removed iteratively until all retained predictors were below this threshold. Because latitude and longitude are spatial surrogates for several unmeasured environmental gradients, their effects should be interpreted cautiously and not as direct causal mechanisms.

Model significance was assessed with 999 unrestricted Monte Carlo permutations. Adjusted R2 was calculated to account for the number of explanatory variables. For each predictor, the ratio of the first constrained eigenvalue to the first unconstrained eigenvalue ($\lambda 1/\lambda 2$) was calculated as an exploratory indicator of predictive strength (Juggins, 2013). Marginal and conditional contributions were assessed to distinguish the variance explained by single predictors from their unique contribution within multivariable models.

Pearson correlation coefficients were calculated between selected pollen percentages and water depth for the 0-35 m marine depth interval. This restricted interval excludes the deeper and hydrodynamically distinctive Bohai Strait channel and is intended to describe the main basin-wide nearshore-offshore gradient. All statistical tests were two-tailed, with $\alpha = 0.05$. Ordination diagrams were produced using R software.

4 Data description

4.1 Sample characteristics and count quality

The dataset contains 534 samples, consisting of 430 marine and 104 riverine surface-sediment samples. Identified pollen grains per sample range from 59 to 1530, with a mean of 397. Four riverine samples and six marine samples contain fewer than 100 identified pollen grains. These low-count samples are retained because they document real low-pollen depositional settings, but they should be flagged during quantitative analyses and treated with caution when interpreting rare taxa. Mean pollen counts are similar in the two subsets, with 406 grains per riverine sample and 395 grains per marine sample.

Low pollen counts are concentrated mainly in Bohai Bay and the Luanhe River estuary (Fig. 2), where high sedimentation rates, coarser grain sizes, or oxidation may dilute or degrade palynomorphs (Yang et al., 2019a). Across the full dataset, 78 % of samples contain 300-600 identified pollen grains, providing stable percentage estimates for the dominant taxa and enabling comparison among regions (Heiri and Lotter, 2001). Users interested in rare taxa should, however, account for count-size effects.

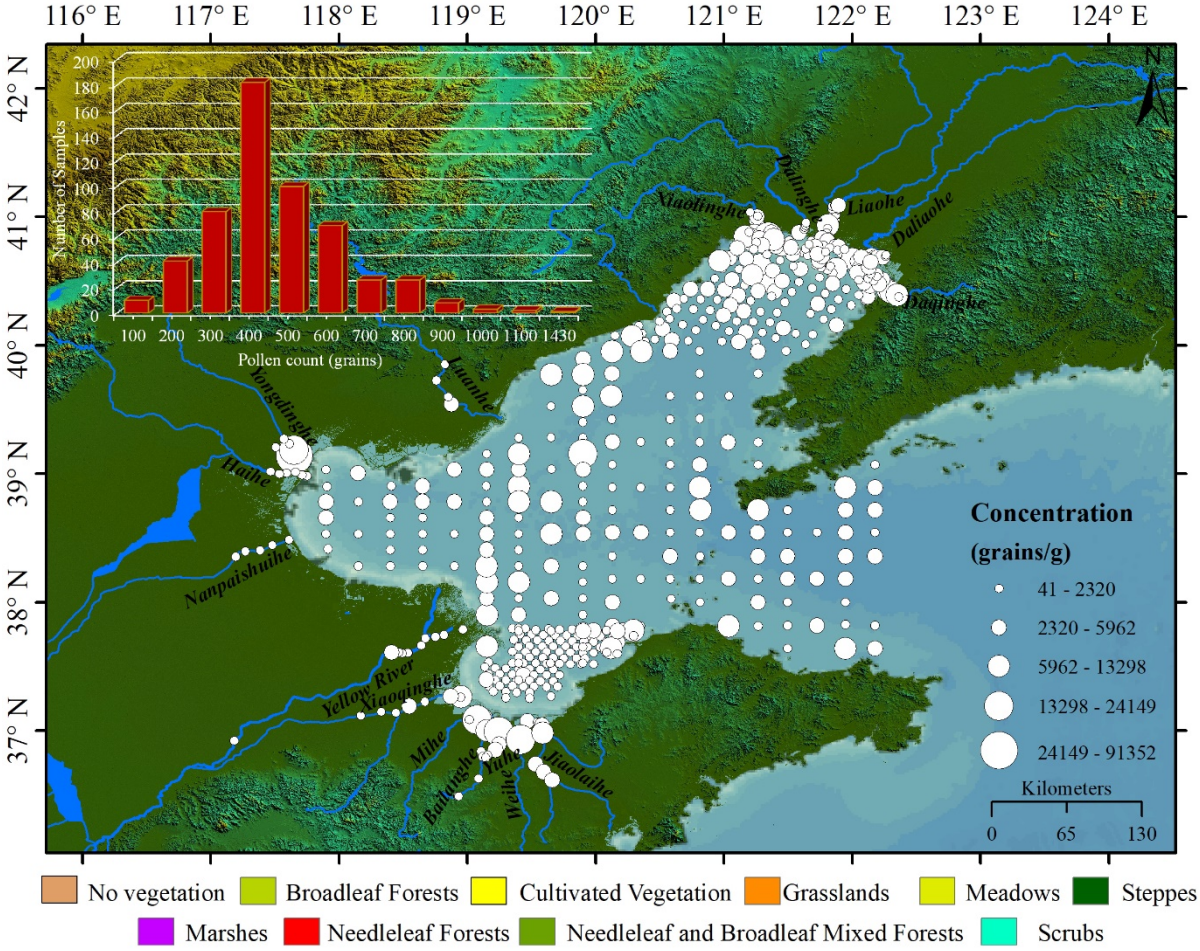

Figure 2. The histogram shows the frequency distribution of pollen-spore sums, and the spatial distribution of pollen-spore concentration. Symbol size represents the different pollen concentration sum, and the inset histogram shows the frequency distribution.

A total of 104 pollen and spore morphotypes were identified. Riverine samples contain 87 morphotypes, whereas marine samples contain 95 morphotypes. Among the 16 rivers, the Daqinghe has the highest richness (52 morphotypes) and the Weihe the lowest (23 morphotypes) (Fig. 3a). The Yellow River contains 39 morphotypes despite its large drainage area and sediment load, possibly reflecting long-distance mixing and dilution by regionally sourced sediment and pollen (Chmura and Liu, 1990; Shen et al., 2006). Because richness values are not standardized by sample number or count size, they should be interpreted descriptively rather than as direct diversity estimates.

Arboreal pollen richness is lower in riverine samples (42 taxa) than in marine samples (50 taxa), whereas herbaceous pollen and fern-spore richness are broadly comparable between the two subsets (Fig. 3b). This pattern is consistent with the preferential atmospheric transport of buoyant bisaccate *Pinus* grains to offshore settings and with stronger local representation of herbaceous taxa in riverine and nearshore environments (Heusser, 1988; Dupont and Wyputta, 2003). Mean pollen concentration is higher in riverine samples (3531 grains g^{-1}) than in marine samples (2419 grains g^{-1}), consistent with proximity to terrestrial pollen sources and dilution by marine sediment accumulation (Naughton et al., 2007).

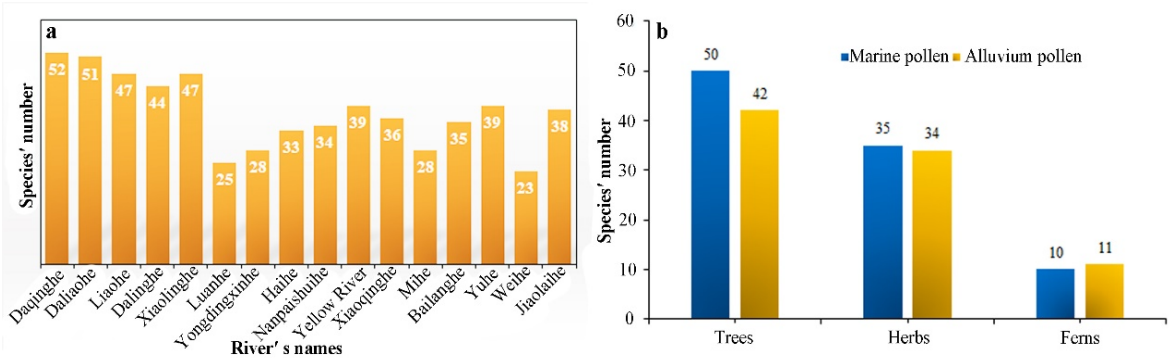

Figure 3. Recorded taxonomic richness in the riverine and marine subsets. (a) Number of pollen and spore morphotypes recorded in each inflowing river; (b) pooled numbers of arboreal, herbaceous, and fern-spore morphotypes in marine and riverine samples. Richness values are descriptive and are not standardized for sample number or count size.

4.2 Spatial distribution of major pollen taxa

Major pollen groups show clear spatial organization across the Bohai Sea and its inflowing rivers (Fig. 4). These patterns provide an internal plausibility check for the dataset because taxa expected to have different production, transport, and depositional behaviour occupy different parts of the land-sea gradient.

Arboreal pollen (AP) is abundant across most marine stations, except in Bohai Bay where non-arboreal pollen is more prominent. AP ranges from 12 % to 98 % and generally exceeds 50 % in offshore samples. The main arboreal components are *Pinus*, *Quercus*, and Betulaceae.

Pinus is the dominant arboreal taxon in marine sediments, with a mean abundance of AP proximately 59 % and a maximum of 98 %. Its distribution closely follows total AP, with the highest values in the deeper Central Basin and Bohai Strait. This pattern is consistent with the high production, buoyancy and preservation potential of bisaccate *Pinus* pollen, which is enriched offshore by both long-distance atmospheric transport and greater hydrodynamic transport efficientcy relative to non-saccate herbaceous taxa (Heusser and Balsam, 1977; Heusser, 1988; Mudie and McCarthy, 2006). *Quercus* is common but subordinate, with a mean abundance of 1.7 % and a maximum of 10.6 %. Higher values occur mainly in the Laotieshan Channel and nearshore areas of northern Liaodong Bay and Laizhou Bay, where fluvial input and coastal currents may deliver non-saccate oak pollen from adjacent peninsulas. Betulaceae pollen is also relatively low, with a mean abundance of 3.3 % and a maximum of about 10.6 %. Its spatial pattern resembles that of *Quercus*, with somewhat higher values in nearshore zones of Liaodong Bay and Laizhou Bay.

Non-arboreal pollen (NAP) ranges from 1.5 % to 88 %. It is enriched in nearshore environments, especially northern Liaodong Bay, Bohai Bay, Laizhou Bay, and the northern Bohai Strait, and is depleted in the Central Basin. This pattern is consistent with local fluvial and coastal-plain inputs from salt marshes, grasslands, and agricultural areas bordering the Bohai Sea (Yang et al., 2016a, 2019a). Among herbaceous taxa, Chenopodiaceae/Amaranthaceae-type is the most abundant group (maximum 59 %, mean 14 %) and closely tracks the distribution of total herbaceous pollen. It is concentrated in nearshore and estuarine settings where halophytic communities occur on saline-alkaline coastal soils (Wang, 1993; Li et al., 2020). *Artemisia*, Poaceae, *Typha*, and Cyperaceae show broadly similar nearshore patterns, supporting the interpretation that nearshore environments are primary sinks for locally derived herbaceous pollen.

Fern spores are relatively abundant in the muddy Central Basin, Bohai Bay, and Liaodong Bay and

reach a maximum of 84 % of total palynomorphs. The main spore groups are *Selaginella*, *Osmunda*, Monoletes, and Triletes, with *Selaginella* dominant. Their association with fine-grained depositional areas is consistent with hydrodynamic sorting and preferential settling in low-energy settings (Traverse, 2007).

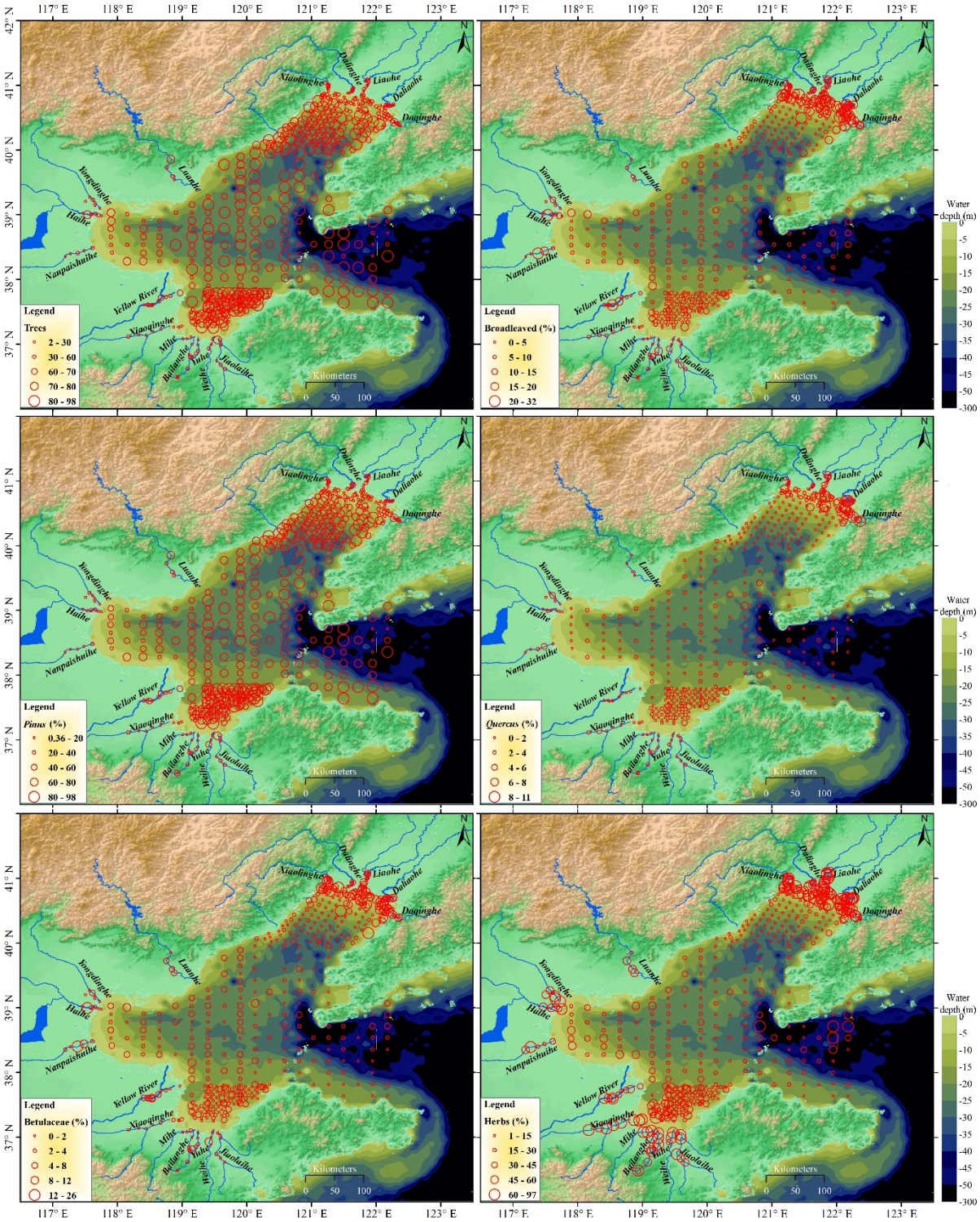

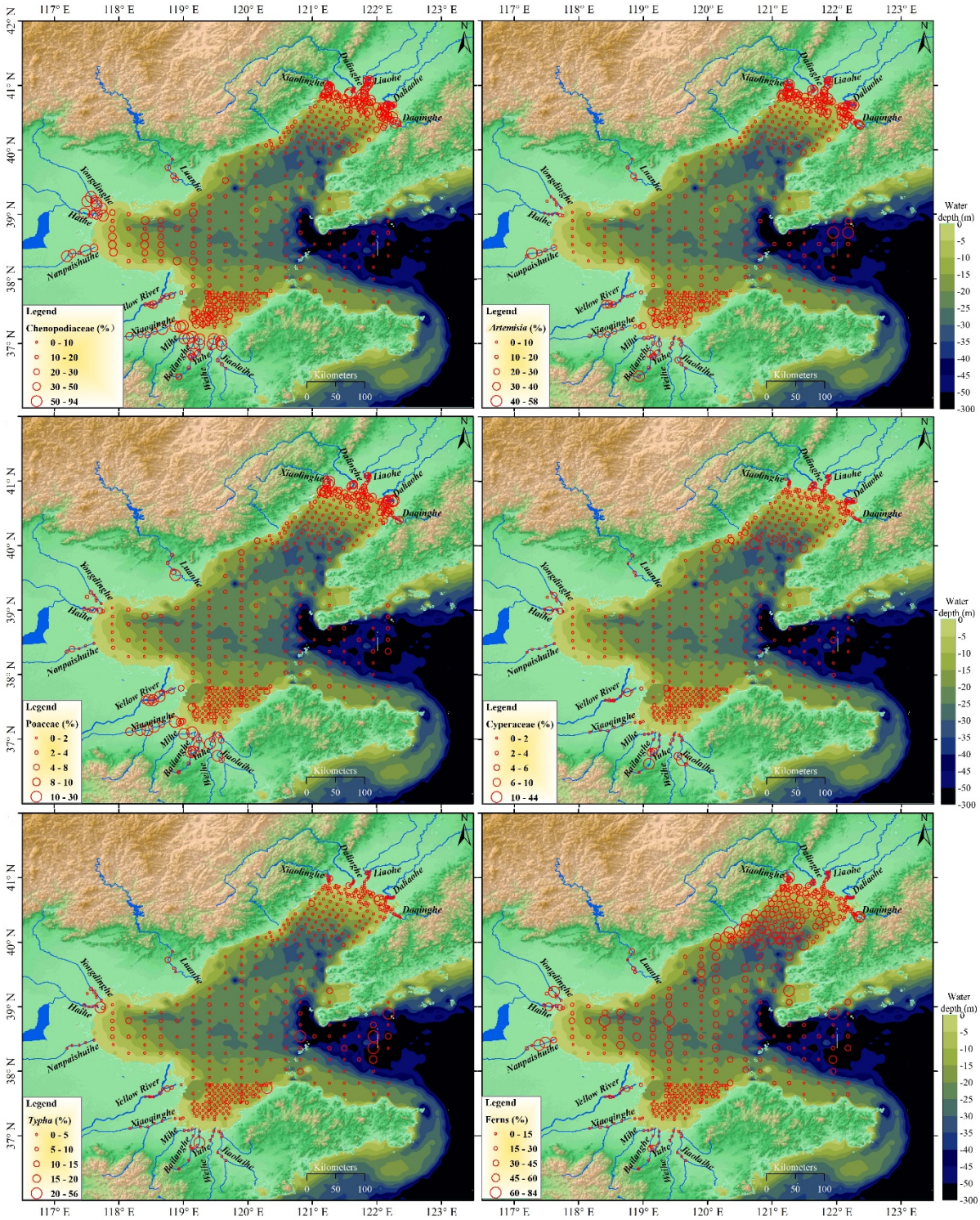

Figure 4. Spatial distributions of major pollen taxa, fern-spore groups, and ecological sums in the Bohai Sea and inflowing rivers.

4.3 Multivariate ordination and environmental controls

4.3.1 Riverine pollen assemblages

Initial VIF diagnostics for the six riverine predictors showed strong multicollinearity (Table 2; Fig. 5a). Sediment load had the highest initial VIF (92.41) and was removed first. Watershed area remained collinear after recalculation (VIF = 23.90) and was also excluded. The final RDA retained latitude (VIF

= 2.02), longitude (2.08), pollen concentration (1.03), and water discharge (1.08).

The final riverine RDA was significant (pseudo-F = 6.393, permutation p = 0.001) and explained 20.53 % of the variance in pollen composition (adjusted R^2 = 0.173). The first two constrained axes accounted for 9.32 % and 6.09 % of total inertia, respectively, representing 75.1 % of the constrained inertia (Fig. 5b). These values indicate that the principal structured gradients are captured by the ordination, although most variance remains unexplained, as expected for multi-source pollen data.

RDA1 separates samples associated with positive latitude, longitude, and water discharge from samples with higher pollen concentration. RDA2 primarily contrasts latitude and longitude. *Selaginella*, *Corylus*, *Betula*, *Typha*, *Quercus*, and *Artemisia* plot toward positive RDA1 scores, whereas Chenopodiaceae/Amaranthaceae-type, Taxodiaceae, Monoletes, and Triletes plot toward negative RDA1 scores. Along RDA2, Monoletes, Taxodiaceae, *Selaginella*, *Typha*, and Liliaceae trend positively, whereas Poaceae, Aster, *Quercus*, *Artemisia*, and Cyperaceae trend negatively.

River groups are separated in ordination space. Yongdingxinhe, Haihe, and Nanpaishuihe plot in the upper part of the diagram; Daqinghe, Daliaohe, Liaohe, Dalinghe, and Xiaolinghe occur mainly on the positive side of RDA1; and Xiaoqinghe, Mihe, Bailanghe, Yuhe, Weihe, and Jiaolaihe occur mainly on the negative side. This pattern is consistent with a geographic gradient around the Bohai Rim, from the cooler Liaodong region to the warmer Shandong region.

The single-predictor λ1/λ2 ranking is longitude (0.234) approximately equal to latitude (0.234), followed by water discharge (0.129), pollen concentration (0.119), sediment load (0.115), and watershed area (0.112). The high ranking of latitude and longitude should be interpreted as evidence that spatially structured environmental and vegetation gradients are important, not that coordinates themselves are mechanistic drivers. Although sediment load and watershed area explain variance when fitted alone, they are redundant in the multivariable model because of collinearity with other basin-scale variables.

Table 2. VIF screening and exploratory RDA results. 'Explained alone' is the variance explained when a variable is fitted as the sole constraint; 'marginal contribution' is the unique contribution of the variable within the final multivariable model.

Subset	Environmental variable	VIF (initial)	VIF (final)	λ1/λ2	Sole predictor: explained variance (%)	Marginal contribution in final RDA: explained variance (%)	*p*-value
Rivers	Latitude	3.06	2.02	0.23	7.53	6.28	0.002
	Longitude	3.17	2.08	0.23	7.52	6.31	0.002
	Concentration	1.04	1.03	0.12	3.54	2.48	0.008
	Area	27.66	—	0.11	3.48	—	—
	Water discharge	79.70	1.08	0.13	3.89	3.53	0.002
	Sediment load	92.41	—	0.11	3.52	—	—
Marine	Longitude	3.52	3.49	0.21	10.92	4.53	0.005
	Latitude	2.45	2.43	0.10	5.18	1.92	0.005
	Depth	1.26	1.26	0.30	12.92	9.40	0.005
	Sand	513.78	—	0.02	1.22	—	—

Subset	Environmental variable	VIF (initial)	VIF (final)	λ1/λ2	Sole predictor: explained variance (%)	Marginal contribution in final RDA: explained variance (%)	*p*-value
	Silt	344.96	2.46	0.03	1.62	1.32	0.005
	Clay	101.63	2.30	0.06	2.98	1.13	0.01
	Mz	22.91	—	0.03	1.61	—	—
	Concentration	1.24	1.23	0.03	1.39	0.26	0.295

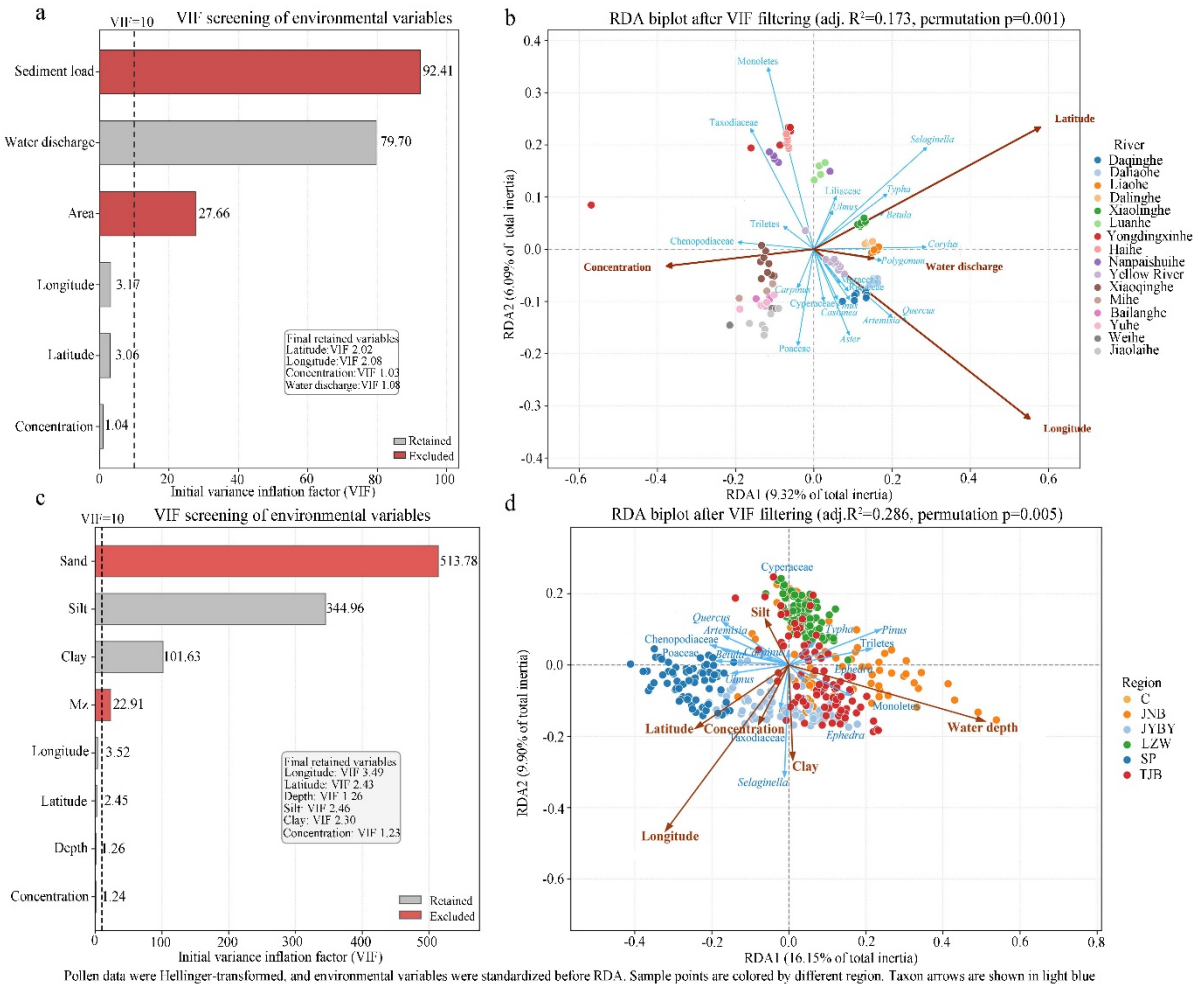

Figure 5. Variance inflation factor (VIF) screening and redundancy analysis (RDA). (a) Initial VIF values for river variables; (b) river RDA biplot using retained variables; (c) initial VIF values for marine variables; (d) marine RDA biplot using retained variables.

4.3.2 Marine pollen assemblages

The marine predictors also showed strong multicollinearity among grain-size variables (Table 2; Fig. 5c). Initial VIF values were high for sand (513.78), silt (344.96), clay (101.63), and mean grain size Mz (22.91), reflecting the mathematical dependence among textural fractions. Sand and mean grain size were therefore removed. The final marine RDA retained longitude (VIF = 3.49), latitude (2.43), water depth (1.26), silt (2.46), clay (2.30), and pollen concentration (1.23).

The final marine RDA was significant (R^2 = 0.296, adjusted R^2 = 0.286, pseudo-F = 30.167, permutation p = 0.005). The retained predictors together explained 29.6 % of the variance in marine pollen composition. RDA1 and RDA2 explained 16.15 % and 9.90 % of total inertia, respectively, corresponding to 88.08 % of constrained inertia (Fig. 5d). The explained fraction is substantial for a large modern surface-sediment dataset, but the residual variance indicates that additional unmeasured factors, including seasonal winds, episodic floods, resuspension, and preservation, also influence pollen assemblages.

Regional sample groups are partly separated in the RDA biplot. Bohai Strait samples plot mainly on the negative side of RDA1, Liaodong Bay samples plot mainly toward positive RDA1 scores, Laizhou Bay samples tend toward higher RDA2 scores, and southern Bohai samples tend toward lower RDA2 scores. Bohai Bay and Central Basin samples occupy more central positions (Fig. 5d), reflecting mixed influences from fluvial input, sediment texture, and basin circulation.

Water depth is aligned mainly with positive RDA1 and negative RDA2, whereas longitude points toward negative values on both axes. Latitude and pollen concentration are also associated with negative RDA1. Silt aligns with positive RDA2 and clay with negative RDA2. The λ1/λ2 ranking of retained predictors is water depth (0.303), longitude (0.214), latitude (0.099), clay (0.055), silt (0.033), and pollen concentration (0.029). Water depth is therefore the strongest retained gradient in the marine data, followed by geographic position and, more weakly, sediment texture. Pollen concentration has a low and non-significant marginal contribution (Table 2) and should not be overinterpreted as an independent predictor in the marine model.

Taxon positions support the spatial patterns described above. *Pinus* and Triletes plot toward deeper-water settings, whereas Chenopodiaceae/Amaranthaceae-type and *Artemisia* plot toward nearshore and river-influenced settings. *Quercus* and Poaceae occupy intermediate positions. This configuration is consistent with buoyant bisaccate pollen, which is enriched offshore by atmospheric transport and hydrodynamic sorting, contrasting with herbaceous taxa delivered mainly by proximal fluvial transport and preferentially deposited nearshore.

5 Technical validation, uncertainty, and usage notes

5.1 Internal validation of pollen-environment relationships

The principal quality check for this dataset is the internal consistency between pollen assemblages, depositional setting, grain size, and water depth. In the marine subset, RDA identifies water depth as the strongest retained predictor (Table 2). Because most Bohai Sea depositional environments occur within 0-35 m water depth and deeper sites are concentrated in the hydrodynamically energetic Laotieshan Channel, the pollen-depth relationship was evaluated primarily within the 0-35 m interval.

Within this interval, *Pinus* percentages increase significantly with water depth, whereas *Quercus*, total herbaceous pollen, Chenopodiaceae/Amaranthaceae-type, and *Artemisia* decrease (Fig. 6). The apparent increase in total AP along this gradient is driven almost entirely by *Pinus*, which dominates the arboreal sum, whereas the other two main arboreal taxa, *Quercus* and Betulaceae, decrease with water depth. The direction of these relationships is consistent with the expected transition from nearshore fluvial and coastal-plain inputs to more distal aeolian influence. The results therefore provide an internal plausibility test for the paired marine-fluvial design, rather than a direct calibration of absolute palaeo-water depth.

The shallow nearshore-estuarine end member (approximately 0-15 m water depth) is characterized by greater influence from rivers, floodplains, salt marshes, deltaic wetlands, and agricultural coastal

plains (Yang et al., 2016a, 2016b, 2016c, 2019a). In this setting, *Quercus* and non-arboreal taxa such as *Artemisia*, Chenopodiaceae/Amaranthaceae-type, Poaceae, and Cyperaceae are relatively enriched because they are delivered mainly by short-distance fluvial and coastal transport.

The deeper central-basin end member (approximately 15-35 m water depth) receives a larger proportional contribution from buoyant saccate pollen. With increasing depth and distance from major river mouths, the fluvial signal is diluted by transport, sorting, resuspension, and sediment focusing, and high-production bisaccate *Pinus* pollen is increasingly overrepresented offshore because of bosht long-distance atmospheric transport and its lower settling velocity in the water column, which allows hydrodynamic transport farther from the coast (Hopkins, 1950; Heusser, 1983, 1988; Chmura et al., 1999; Dupont and Wyputta, 2003; Mudie and McCarthy, 2006; Traverse, 2007).

The dataset agrees with marine palynological theory and previous Bohai Sea studies showing that *Pinus* and fern spores increase toward deeper waters and that river input, basin circulation, and fine-grained sediment deposition shape the spatial distribution of pollen assemblages (Wang, 1993; Yang et al., 2016c, 2019, 2021). Its added value is the explicit pairing of the marine samples with fluvial samples from the same source-to-sink system, which allows users to compare source-area assemblages with marine depositional assemblages directly.

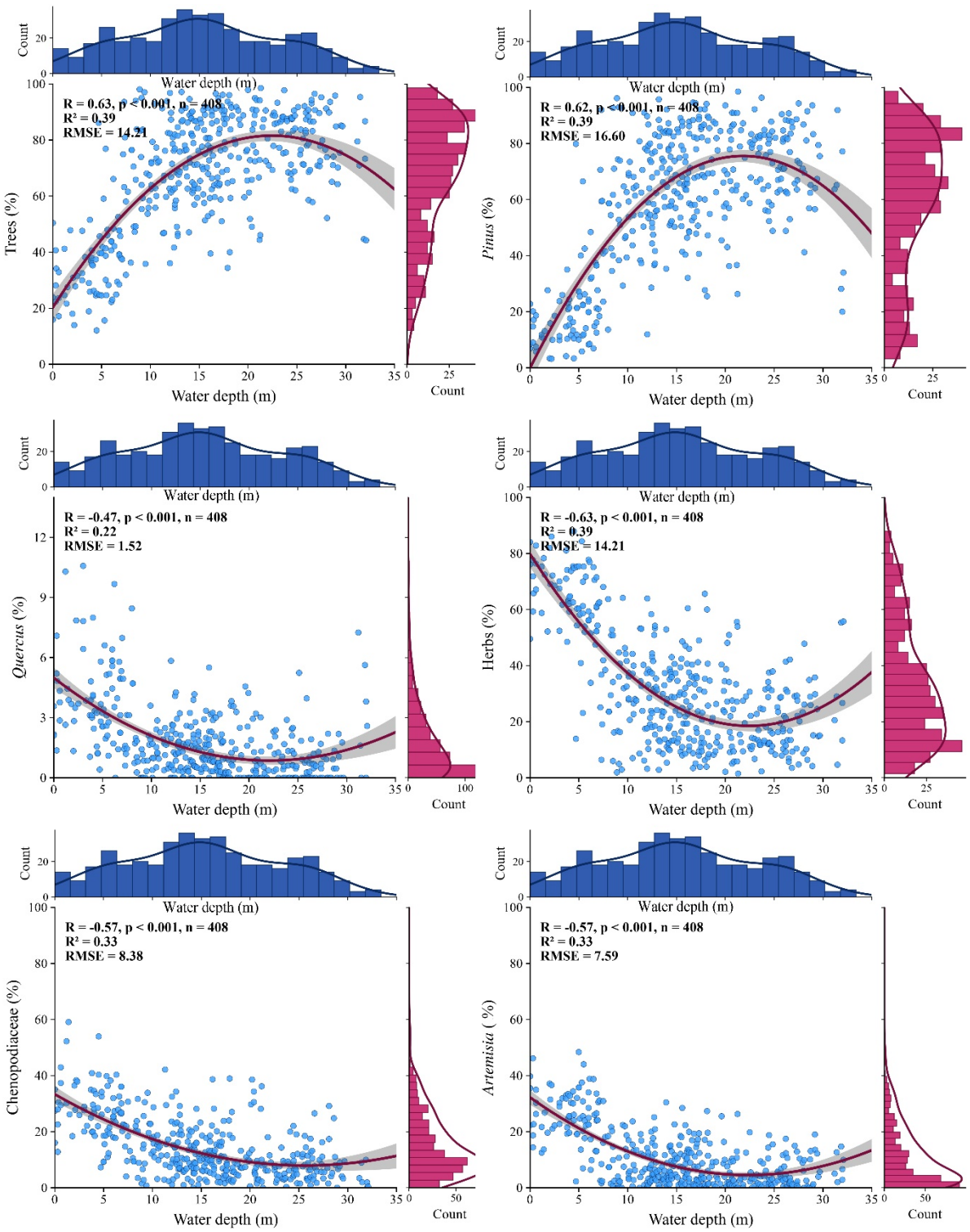

Figure 6. Relationships between water depth (0-35 m) and the percentages of total arboreal pollen, *Pinus*, *Quercus*, total herbaceous pollen, Chenopodiaceae/Amaranthaceae-type, and *Artemisia*. Reported r values are Pearson correlation coefficients.

5.2 Recommended applications and limitations

The dataset can be used as a modern analogue for evaluating how relative shoreline distance and river-mouth proximity influence pollen spectra in the Bohai-Yellow Sea region (Zheng et al., 2011, 2013; Li et al., 2020). Its strongest application is not the direct reconstruction of water depth but the

identification of assemblage tendencies associated with fluvial-dominated nearshore settings versus more distal, aeolian-influenced marine settings.

Water depth in the modern dataset should therefore not be treated as a simple fossil sea-level variable. Instead, it is a spatial proxy for a suite of covarying factors, including distance from shore, distance from river mouths, sediment texture, depositional energy, and the relative balance between fluvial and atmospheric pollen transport. During lowstands, shorelines and river mouths move basinward and exposed shelf areas may contribute local herbaceous, wetland, and freshwater signals to marginal-marine deposits (Zheng et al., 2011, 2013). During highstands, greater source-to-sink distance generally reduces direct fluvial pollen delivery and increases the relative contribution of long-distance aeolian pollen.

In fossil records, intervals resembling the shallow nearshore end member may show lower *Pinus* percentages, lower ratios of arboreal pollen to non-arboreal pollen (AP/NAP), of *Pinus* to *Artemisia* (P/A), and of bladder-bearing pollen to non-arboreal pollen (PB/NAP), together with higher proportions of *Artemisia*, Chenopodiaceae/Amaranthaceae-type, Poaceae, Cyperaceae, aquatic pollen and freshwater algae. Intervals resembling the deeper offshore end member may show higher *Pinus* percentages, higher AP/NAP, P/A, and PB/NAP ratios, lower herbaceous representation, finer-grained offshore muds, and more open-marine microfossil indicators. These criteria should be used together rather than individually.

Published records from the deep-water Okinawa Trough illustrate that pollen assemblages respond sensitively to coupled sea-level and vegetation changes, although the underlying mechanisms differ from those in the shallow Bohai Sea. Core DGKS9602 (28°07.5′N, 127°22.1′E; water depth 988 m) and core MD98-2194 (Middle Okinawa Trough; 989 m water depth) are located far from any shoreline, even during glacial lowstands when sea level was 120-130 m lower. Pollen records from the Okinawa Trough show that pollen assemblages exhibit regular alternating patterns between glacial and interglacial periods. During interglacials, saccate conifer pollen, represented by *Pinus* and *Tsuga*, overwhelmingly dominates. This high abundance corresponds to high sea-level stands, when pollen is primarily derived from distant landmasses and transported over long distances by wind. In glacial stages, the contents of herbaceous pollen (e.g., *Artemisia*, Cyperaceae, Poaceae) and freshwater algae increase markedly. Particularly during the Last Glacial Maximum, when the shelf was largely exposed and the coastline retreated substantially, rivers could no longer supply sediment directly to the Okinawa Trough. Instead, the grassland and meadow vegetation developed on the exposed shelf became an important pollen source for the trough during glacial periods, leading to a significant increase in herbaceous pollen such as *Artemisia* and Chenopodiaceae in the trough sediments—a pattern that shows a strong negative correlation with sea-level changes (Zheng et al., 2011, 2013). on glacial–interglacial timescales, the primary factor governing changes in sedimentary pollen assemblages and provenance in the Okinawa Trough or deep-sea basins is shoreline migration caused by sea-level fluctuations, and its signal intensity even exceeds that of climatic changes in the source areas themselves.Therefore, the P/A and PB/NAP variations in these cores therefore can be interpreted as an inferred measure of shoreline distance. Organic geochemical evidence from the Okinawa Trough also records reduced terrestrial plant input as the shoreline retreated during deglaciation (Ujiié et al., 2001). These deep-water records nonetheless confirm that pollen assemblages track land-sea reorganization on glacial-interglacial timescales, which is the same principle that underpins the application of our shallow-water modern dataset to the Bohai-Yellow Sea region.

The Bohai Sea is especially sensitive to shoreline displacement because of its shallow bathymetry

and large fluvial inputs. A glacial sea-level fall of approximately 120-130 m would expose the present Bohai Sea and much of the adjacent shelf (Yokoyama et al., 2000; Lambeck and Chappell, 2001; Lambeck et al., 2014). Consequently, down-core pollen records from the region should be interpreted as combined signals of vegetation change, climate variability, source-area migration, river routing, shelf exposure, and depositional environment.

For practical reuse, pollen-based shoreline-proximity indicators should be cross-checked against pollen concentration, grain size, sedimentary facies, freshwater algae such as *Pediastrum* and *Botryococcus*, dinoflagellate cysts, foraminifera, geochemical proxies, and independent chronological control. Samples with low pollen sums or strong evidence of reworking should be analysed separately or excluded from transfer-function development.

The main limitations of the dataset are that surface sediments are intermingled with limited relict deposits that were not investigated in sufficient detail; river sampling emphasizes lower reaches and estuaries rather than the full upstream catchment; coordinates and hydrological variables cannot represent all ecological gradients; and pollen percentages are compositional data influenced by both production and transport. Monsoon wind strength may also vary independently of sea level (An, 2000; Sun et al., 2012), potentially altering aeolian pollen flux. These limitations do not reduce the value of the dataset, but they define the conditions under which it should be reused.

6 Code and data availability

The dataset includes pollen count data of each sample, as well as geographic coordinate, water depth, as well as the grain size composition. The dataset is openly accessible from the National Tibetan Plateau / Third Pole Environment Data Center (TPDC; Li and Yang, 2026; https://doi.org/10.11888/Paleoenv.tpdc.303516).

7 Summary

We present a paired modern marine-fluvial pollen dataset for the Bohai Sea region, comprising 430 marine surface-sediment samples and 104 fluvial surface-sediment samples from 16 inflowing rivers. The dataset records 104 pollen and spore morphotypes, associated sample metadata, pollen concentrations, and grain-size variables. Marine pollen assemblages are dominated by *Pinus*, especially in deeper and more distal settings, whereas nearshore and river-influenced assemblages contain higher proportions of herbaceous taxa such as Chenopodiaceae/Amaranthaceae-type and *Artemisia*. Exploratory RDA shows that water depth is the strongest retained marine predictor, while riverine assemblages are structured mainly by geographic position, water discharge, and pollen concentration. The 0-35 m depth gradient provides an internally consistent modern analogue for distinguishing fluvial-dominated nearshore pollen assemblages from more aeolian-influenced offshore assemblages. The dataset is suitable for reuse in palaeoenvironmental research, especially for assessing source-to-sink processes and shoreline-proximity effects in Bohai-Yellow Sea sediment cores, provided that users account for the stated uncertainties and validate interpretations with independent proxies.

Author contributions

J. Li designed the pollen dataset, S. Ye, X. Mei, X. Cao, X. Meng, M. Gao, B. Chen. collected the samples, S. Yang performed pollen extraction and identification. S. Yang, Q. Hao., S. Yi, and M. Guang compiled the standardization for the dataset, performed numerical analyses, and organized the

manuscript. All authors discussed the results and contributed to the final paper.

Competing interests

The corresponding author declares that none of the authors has any competing interests.

Acknowledgements

This study was jointly funded by the Shandong Provincial Natural Science Foundation, China (Grant No. ZR2024MD037), National Natural Science Foundation of China (NSFC, Grants Nos. 41876057, 41506062), China Geological Survey projects (Grant Nos. DD202607102003, DD2026031026), and the UN Decade of Ocean Science for Sustainable Development 2021-2030 (the action of No. 66.8) of ONCE programme. We thank Prof. Zhongbo Wang and Dr. Jun Sun for their insightful discussions and suggestions on this work. We are grateful to two anonymous reviewers and the editor for their constructive comments, which significantly improved this paper.

References

An, Z. S.: The history and variability of the East Asian paleomonsoon climate, Quat. Sci. Rev., 19, 171–187, https://doi.org/10.1016/S0277-3791(99)00060-8, 2000.

Berglund, B. E. and Ralska-Jasiewiczowa, M.: Pollen analysis and pollen diagrams, in: Handbook of Holocene Palaeoecology and Palaeohydrology, edited by: Berglund, B. E., Wiley, Chichester, 455–484, 1986.

Blanchet, F. G., Legendre, P., and Borcard, D.: Forward selection of explanatory variables, Ecology, 89, 2623–2632, https://doi.org/10.1890/07-0986.1, 2008.

Blott, S. J. and Pye, K.: GRADISTAT: a grain size distribution and statistics package for the analysis of unconsolidated sediments, Earth Surf. Proc. Land., 26, 1237–1248, https://doi.org/10.1002/esp.261, 2001.

Brush, G. S., Brush, L. M., and Traverse, A.: Transport and deposition of pollen in an estuary: signature of the landscape. Sedimentation of organic particles. Cambridge University Press, Cambridge, 33-46, 1994.

Chen, M. T., Shiau, L. J., Yu, P. S., Chiu, T. C., Chen, Y. G., and Wei, K. Y.: 500 000-Year records of carbonate, organic carbon, and foraminiferal sea-surface temperature from the southeastern South China Sea (near Palawan Island). Palaeogeogr. Palaeoclimatol. Palaeoecol., 197(1-2), 113-131, https://doi.org/10.1016/S0031-0182(03)00389-4, 2003.

Chen, Z., Wu, S., and Xia, D.: The Bay Chorography in China. Ocean Press, Beijing, 1998. (in Chinese)

Chmura, G. L. and Liu, K.-B.: Pollen in the lower Mississippi River, Rev. Palaeobot. Palynol., 64, 253–261, https://doi.org/10.1016/0034-6667(90)90140-E, 1990.

Chmura, G. L., Smirnov, A., and Campbell, I. D.: Pollen transport through distributaries and depositional patterns in coastal waters, Palaeogeogr. Palaeoclimatol. Palaeoecol., 149, 257–270, https://doi.org/10.1016/S0031-0182(98)00205-3, 1999.

Davis, B. A. S., Zanon, M., Collins, P., Mauri, A., Bakker, J., Barboni, D., Barthelmes, A., Beaudouin, C., Bjune, A. E., Bozilova, E., Bradshaw, R. H. W., Brayshay, B. A., Brewer, S., Brugiapaglia, E., Bunting, J., Connor, S. E., de Beaulieu, J.-L., Edwards, K., Ejarque, A., Fall, P., Florenzano, A., Fyfe, R., Galop, D., Giardini, M., Giesecke, T., Grant, M. J., Guiot, J., Jahns, S., Jankovská, V., Juggins, S., Kahrmann, M., Karpińska-Kołaczek, M., Kołaczek, P., Kühl, N., Kuneš, P., Lapteva, E. G., Leroy, S. A. G., Leydet, M., López Sáez, J. A., Masi, A., Matthias, I., Mazier, F., Meltsov,

V., Mercuri, A. M., Miras, Y., Mitchell, F. J. G., Morris, J. L., Naughton, F., Nielsen, A. B., Novenko, E., Odgaard, B., Ortu, E., Overballe-Petersen, M. V., Pardoe, H. S., Peglar, S. M., Pidek, I. A., Sadori, L., Seppä, H., Severova, E., Shaw, H., Święta-Musznicka, J., Theuerkauf, M., Tonkov, S., Veski, S., van der Knaap, W. O., van Leeuwen, J. F. N., Woodbridge, J., Zimny, M., and Kaplan, J. O.: The European Modern Pollen Database (EMPD) project, Veg. Hist. Archaeobot., 22, 521–530, https://doi.org/10.1007/s00334-012-0388-5, 2013.

Dupont, L. M. and Wyputta, U.: Reconstructing pathways of aeolian pollen transport to the marine sediments along the coastline of SW Africa, Quat. Sci. Rev., 22, 157–174, https://doi.org/10.1016/S0277-3791(02)00032-X, 2003.

Editorial Committee of Encyclopedia of Rivers and Lakes in China.: Encyclopedia of Rivers and Lakes in China. Beijing, China Water Power Press, 2014. (in Chinese),

Fang, G., Kwok, Y. K., Yu, K., and Zhu, Y.: Numerical simulation of principal tidal constituents in the South China Sea, Gulf of Tonkin and Gulf of Thailand, Cont. Shelf Res., 19, 845–869, https://doi.org/10.1016/S0278-4343(99)00002-3, 1999.

Guan, B.: Patterns and structures of the currents in Bohai, Huanghai and East China Seas, Springer Netherlands, Dordrecht, 17–26, 1994.

Havinga, A. J.: A 20-year experimental investigation into the differential corrosion susceptibility of pollen and spores in various soil types, Pollen et Spores, 26, 541–558, 1984.

Heiri, O. and Lotter, A. F.: Effect of low count sums on quantitative environmental reconstructions: an example using subfossil chironomids, J. Paleolimnol., 26, 343–350, https://doi.org/10.1023/A:1017568913302, 2001.

Heusser, L. and Balsam, W. L.: Pollen distribution in the northeast Pacific Ocean, Quat. Res., 7, 45–62, https://doi.org/10.1016/0033-5894(77)90013-8, 1977.

Heusser, L. E.: Pollen distribution in marine sediments on the continental margin off northern California, Mar. Geol., 80, 131–147, https://doi.org/10.1016/0025-3227(88)90076-X, 1988.

Heusser, L. E.: Pollen distribution in the bottom sediments of the western North Atlantic Ocean, Mar. Micropaleontol., 8, 77–88, https://doi.org/10.1016/0377-8398(83)90006-3, 1983.

Hill, M. O. and Gauch, H. G.: Detrended correspondence analysis: an improved ordination technique, Vegetatio, 42, 47–58, https://doi.org/10.1007/BF00048870, 1980.

Hopkins, J. S.: Differential flotation and deposition of coniferous and deciduous tree pollen. Ecology, 31(4), 633-641, https://doi.org/10.2307/1931580, 1950.

IBSCIBAS (Institute of Botany and South China Institute of Botany, Academia Sinica): Angiosperm Pollen Flora of Tropic and Subtropic China, Science Press, Beijing, 1985. (in Chinese)

IOCAS (Institute of Oceanology, Chinese Academy of Sciences): Geology of the Bohai Sea, China Ocean Press, Beijing, 1985. (in Chinese)

Juggins, S.: Quantitative reconstructions in palaeolimnology: new paradigm or sick science?, Quat. Sci. Rev., 64, 20–32, https://doi.org/10.1016/j.quascirev.2012.12.014, 2013.

Lambeck, K. and Chappell, J.: Sea level change through the last glacial cycle, Science, 292, 679–686, https://doi.org/10.1126/science.1059549, 2001.

Lambeck, K., Rouby, H., Purcell, A., Sun, Y., and Sambridge, M.: Sea level and global ice volumes from the Last Glacial Maximum to the Holocene, Proc. Natl. Acad. Sci. USA, 111, 15296–15303, https://doi.org/10.1073/pnas.1411762111, 2014.

Legendre, P. and Gallagher, E. D.: Ecologically meaningful transformations for ordination of species data, Oecologia, 129, 271–280, https://doi.org/10.1007/s004420100716, 2001.

Li, J., Yang, S.: A paired marine-fluvial modern pollen dataset from the Bohai Sea and its inflowing rivers, China. National Tibetan Plateau / Third Pole Environment Data Center [data set], https://doi.org/10.11888/Paleoenv.tpdc.303516, 2026.

Li, J., Yang, S., Li, R., Shu, J., Chen, X., Meng, Y., Ye, S., and He, L., 2020. Vegetation history and environment changes since MIS 5 recorded by pollen assemblages in sediments from the western Bohai Sea, Northern China. J. Asian Earth Sci. 187, 104085, https://doi.org/10.1016/j.jseaes.2019.104085, 2020.

Liu, J., Saito, Y., Wang, H., Yang, Z., and Nakashima, R.: Sedimentary evolution of the Holocene subaqueous clinoform off the Shandong Peninsula in the Yellow Sea, Mar. Geol., 236, 165–187, https://doi.org/10.1016/j.margeo.2006.10.031, 2007.

Liu, J., Saito, Y., Wang, H., Zhou, L., and Yang, Z.: Sedimentary evolution of the Holocene subaqueous clinoform off the Shandong Peninsula in the Yellow Sea, Mar. Geol., 264, 101-116, https://doi.org/10.1016/j.margeo.2009.04.016, 2009.

Liu, Z., Xia, D., Berne, S., Wang, K., Marsset, T., Tang, Y., Bourillet, J.F.: Tidal deposition systems of China's continental shelf, with special reference to the eastern Bohai Sea, Mar. Geol., 145, 225–253, https://doi.org/10.1016/s0025-3227(97)00116-3, 1998.

Luo, C., Chen, M., Xiang, R., Liu, J., Zhang, L., Lu, J., and Yang, M.: Modern pollen distribution in marine sediments from the northern part of the South China Sea. Marine Micropaleontology, 108, 41-56. https://doi.org/10.1016/j.marmicro.2014.03.001, 2014.

Meng, G. L. and Wang, S. Q.: Studies on the Quaternary sporo-pollen assemblage from the Bohai Sea drilling core BC-1 and its paleoclimate, Oceanol. Limnol. Sin., 18, 253–264, 1987. (in Chinese)

Milliman, J. D. and Farnsworth, K. L.: River Discharge to the Coastal Ocean: A Global Synthesis, Cambridge University Press, Cambridge, 384 pp., 2011.

Milliman, J. D. and Meade, R. H.: World-wide delivery of river sediment to the oceans, J. Geol., 91, 1–21, https://doi.org/10.1086/628741, 1983.

Ministry of water Resources of China: China river sediment bulletin in 2011. China Water & Power Press, Beijing, 64 pp., 2011. (in Chinese)

Moore, P. D., Webb, J. A., and Collinson, M. E.: Pollen Analysis, 2nd edn., Blackwell Scientific, Oxford, 216 pp., 1991.

Mudie, P. J. and McCarthy, F. M. G.: Marine palynology: potentials for onshore–offshore correlation of Pleistocene–Holocene records, Trans. R. Soc. S. Afr., 61, 139–157, https://doi.org/10.1080/00359190609519964, 2006.

Müller, J.: Palynology of recent Orinoco delta and shelf sediments: reports of the Orinoco shelf expedition, volume 5, Micropaleontology, 5, 1–32, https://doi.org/10.2307/1484153, 1959.

Nakagawa, T., Brugiapaglia, E., Digerfeldt, G., Reille, M., de Beaulieu, J. L., and Yasuda, Y.: Dense-media separation as a more efficient pollen extraction method for use with organic sediment samples: comparison with the conventional method, Boreas, 27, 15–24, https://doi.org/10.1111/j.1502-3885.1998.tb00863.x, 1998.

Naughton, F., Sanchez Goñi, M. F., Desprat, S., Turon, J.L., Duprat, J., Malaizé, B., Joli, C., Cortijo, E., Drago, T., and Freitas, M. C.: Present-day and past (last 25,000 years) marine pollen signal off western Iberia, Mar. Micropaleontol., 62, 91–114, https://doi.org/10.1016/j.marmicro.2006.07.006, 2007.

Oksanen, J., Blanchet, F. G., Friendly, M., Kindt, R., Legendre, P., McGlinn, D., Minchin, P. R., O'Hara, R. B., Simpson, G. L., Solymos, P., Stevens, M. H. H., Szoecs, E., and Wagner, H.: vegan:

Community Ecology Package, R package version 2.5-6, https://CRAN.R-project.org/package=vegan, 2019.
Overpeck, J. T., Webb, T., and Prentice, I. C.: Quantitative interpretation of fossil pollen spectra: dissimilarity coefficients and the method of modern analogs, Quat. Res., 23, 87–108, https://doi.org/10.1016/0033-5894(85)90074-2, 1985.
Prentice, I. C.: Multidimensional scaling as a research tool in Quaternary palynology: a review of theory and methods, Rev. Palaeobot. Palynol., 31, 71–104, https://doi.org/10.1016/0034-6667(80)90023-8, 1980.
Prentice, I. C.: Pollen representation, source area, and basin size: toward a unified theory of pollen analysis, Quat. Res., 23, 76–86, https://doi.org/10.1016/0033-5894(85)90073-0, 1985.
Qin, Y. S., Zhao, Y. Y., Chen, L. R., and Zhao, S. L.: Geology of Bohai Sea, China Ocean Press, Beijing, 1990. (in Chinese)
R Core Team: R: A Language and Environment for Statistical Computing, R Foundation for Statistical Computing, Vienna, Austria, https://www.R-project.org/, 2023.
Ren, G. and Beug, H.-J.: Mapping Holocene pollen data and vegetation of China, Quat. Sci. Rev., 21, 1395–1422, https://doi.org/10.1016/S0277-3791(01)00119-6, 2002.
Shen, C., Liu, K. B., Tang, L., and Overpeck, J. T.: Quantitative relationships between modern pollen rain and climate in the Tibetan Plateau. Review of Palaeobotany and Palynology, 140(1-2), 61-77. https://doi.org/10.1016/j.revpalbo.2006.03.001, 2006.
Stockmarr, J.: Tablets with spores used in absolute pollen analysis, Pollen Spores, 13, 615–621, 1971.
Sun, X., Luo, Y., and Chen, H.: Pollen record of the last 280 ka from deep-sea sediments of the northern South China Sea, Sci. China Ser. D-Earth Sci., 44, 879–888, https://doi.org/10.1007/BF02907079, 2001.
Sun, Y., Clemens, S. C., Morrill, C., Lin, X., Wang, X., and An, Z.: Influence of Atlantic meridional overturning circulation on the East Asian winter monsoon, Nat. Geosci., 5, 46–49, https://doi.org/10.1038/ngeo1326, 2012.
Tang, L., Mao, L., Shu, J., Li, C., Shen, C., and Zhou, Z.: An Illustrated Handbook of Quaternary Pollen and Spores in China, Science Press, Beijing, 2020.
ter Braak, C. J. F. and Prentice, I. C.: A theory of gradient analysis, Adv. Ecol. Res., 18, 271–317, https://doi.org/10.1016/S0065-2504(08)60183-X, 1988.
ter Braak, C. J. F. and Verdonschot, P. F. M.: Canonical correspondence analysis and related multivariate methods in aquatic ecology, Aquat. Sci., 57, 255–289, https://doi.org/10.1007/BF00877430, 1995.
Traverse, A.: Paleopalynology, 2nd edn., Springer, Dordrecht, 813 pp., https://doi.org/10.1007/978-1-4020-5610-9, 2007.
Ujiié, H., Hatakeyama, Y., Gu, X. X., Yamamoto, S., Ishiwatari, R., and Maeda, L.: Upward decrease of organic C/N ratios in the Okinawa Trough cores: proxy for tracing the post-glacial retreat of the continental shore line, Palaeogeogr. Palaeoclimatol. Palaeoecol., 165, 129–140, https://doi.org/10.1016/S0031-0182(00)00157-7, 2001.
Wang, F. X., Qian, N. F., Zhang, Y. L., and Yang, H. Q.: Pollen Flora of China, 2nd edn., Science Press, Beijing, 461 pp., 1995. (in Chinese)
Wang, H. J., Yang, Z. S., Saito, Y., Liu, J. P., Sun, X. X., and Wang, Y.: Stepwise decreases of the Huanghe (Yellow River) sediment load (1950–2005): impacts of climate change and human

activities, Global Planet. Change, 57, 331–354, https://doi.org/10.1016/j.gloplacha.2007.01.003, 2007.

Wang, H. J.: Climate Change Around Bohai Region During 1956 to 2011 and its Relationship with ENSO, M.D. Thesis, Northwest Normal University, 2013. (in Chinese)

Wang, H., Saito, Y., Zhang, Y., Bi, N., Sun, X., and Yang, Z.: Recent changes of sediment flux to the western Pacific Ocean from major rivers in East and Southeast Asia, Earth-Sci. Rev., 108, 80–100, https://doi.org/10.1016/j.earscirev.2011.06.003, 2011.

Wang, K. F.: Spore-Pollen and Algal Assemblages in the Sediments of the Bohai Sea and Palaeoenvironments, Geological Publishing House, Beijing, 157 pp., 1993. (in Chinese).

Wang, P. X., Li, Q. Y., and Tian, J.: Pleistocene paleoceanography of the South China Sea: progress over the past 20 years, Mar. Geol., 352, 381–396, https://doi.org/10.1016/j.margeo.2014.03.003, 2014.

Wang, Y.G., and He, B.L.: Modern erosion and accumulation trends of the north shallow region of Liaodong Bay. Trans. Oceanol. Limnol. (4), 15-21, 1993. (in Chinese)

Wentworth, C. K.: A scale of grade and class terms for clastic sediments, J. Geol., 30, 377–392, https://doi.org/10.1086/622910, 1922.

Yang, D.Z.: Analysis of hydrologic characteristics in the Daqing River basin. Hydrology 23 (2), 58－60, 2003. (in Chinese)

Yang, S., Li, J., Liu, K., Li, R., Wen, Z., Ye, S., Yi, S., and Chen, X.: Pollen-spore distribution in the surface sediments of the western Bohai Sea, China, Quat. Int., 392, 213–223, https://doi.org/10.1016/j.quaint.2015.05.072, 2016a.

Yang, S., Li, J., Mao, L., Liu, K., Gao, M., Ye, S., Yi, S., Zhou, L., and Wang, F.: Assessing pollen distribution patterns and provenance based on palynological investigation on surface sediments from Laizhou Bay, China, Palaeogeogr. Palaeoclimatol. Palaeoecol., 457, 209–220, https://doi.org/10.1016/j.palaeo.2016.06.010, 2016c.

Yang, S., Li, J., Ye, S., Mackenzie, L., Yuan, H., He, L., Zhao, G., Pei, S., and Ding, X.: Pollen distribution and transportation patterns in surface sediments of Liaodong Bay, China. Science of the Total Environment, 771, 144883. https://doi.org/10.1016/j.scitotenv.2020.144883, 2021.

Yang, S., Liu, K., Yi, S., Ye, s., Li, J., Yuan, H., Zhao, G., Pei, S., He, L., Ding, X., and Cho, T.S.: Distribution and provenance of modern pollen and spores in the surface sediments of Liaodong Bay, China, Mar. Geol. 376, 1–14, http://dx.doi.org/10.1016/j.margeo.2016.03.004, 2016b.

Yang, S., Song, B., Ye, S., Laws, E. A., He, L., Li, J., Zhao, G., and Zhao, J.: Large-scale pollen distribution in marine surface sediments from the Bohai Sea, China: insights into pollen provenance, transport, deposition, and coastal-shelf paleoenvironment, Prog. Oceanogr., 178, 102183, https://doi.org/10.1016/j.pocean.2019.102183, 2019a.

Yang, S., Song, B., Ye, S., Xu, Q., He, L., Zhao, G., Li, J., Laes, E.A., Regional-scale distributions of pollen and spore assemblages in alluvium around the Bohai Sea: An essential step toward understanding marine palynological sources in China. Mar. Geol., 415, 105968.https://doi.org/10.1016/j.margeo.2019.105968, 2019b.

Yokoyama, Y., Lambeck, K., De Deckker, P., Johnston, P., and Fifield, L. K.: Timing of the Last Glacial Maximum from observed sea-level minima, Nature, 406, 713–716, https://doi.org/10.1038/35021035, 2000.

Youn, J., and Kim, T. J.: Geochemical composition and provenance of muddy shelf deposits in the East China Sea. Quat. Int., 230(1-2), 3-12. https://doi.org/10.1016/j.quaint.2009.11.001, 2011.

Zhang, D.E., 1991. Historical records of climate change in China. Quat. Sci. Rev. 10, 551-554, https://doi.org/ 10.1016/0277-3791(91)90049-Z, 1991.

Zhang, X. (Ed.): Vegetation Map of the People's Republic of China (1:1,000,000), Geology Press, Beijing, 274 pp., 2007.

Zheng, Z., Huang, K. Y., Deng, Y., Cao, L. L., Yu, S. H., Suc, J.-P., Berné, S., and Guichard, F.: A ~200 ka pollen record from Okinawa Trough: paleoenvironment reconstruction of glacial–interglacial cycles, Sci. China Earth Sci., 56, 1731–1747, https://doi.org/10.1007/s11430-013-4619-0, 2013.

Zheng, Z., Yang, S., Deng, Y., Huang, K., Wei, J., Berné, S., and Suc, J.-P.: Pollen record of the past 60 ka BP in the Middle Okinawa Trough: terrestrial provenance and reconstruction of the paleoenvironment, Palaeogeogr. Palaeoclimatol. Palaeoecol., 307, 285–300, https://doi.org/10.1016/j.palaeo.2011.05.026, 2011.

Zhu, D.Q.: Chinese Water System Dictionary. Qingdao Publishing House, Qingdao, 709pp., 2007. (in Chinese)